Dehumidification of sewage sludge using quonset solar tunnel dryer: An experimental and numerical approach

Dehumidification of sewage sludge using quonset solar tunnel dryer: an experimental and numerical approach

Faraz Afshari[1], Ataollah Khanlari[2], Azim Doğuş Tuncer[3,4*], Adnan Sözen[5], İstemihan Şahinkesen[3], Giovanni Di Nicola[6]

[1]Mechanical Engineering, Faculty of Engineering, Erzurum Technical University, Erzurum, Turkey
[2]Mechanical Engineering, Faculty of Engineering, University of Turkish Aeronautical Association, Ankara, Turkey
[3]Energy Systems Engineering, Faculty of Engineering-Architecture, Burdur Mehmet Akif Ersoy University, Burdur, Turkey
[4]Institute of Natural and Applied Sciences, Gazi University, Ankara, Turkey
[5]Energy Systems Engineering, Faculty of Technology, Gazi University, Ankara, Turkey
[6]Department of Industrial Engineering and Mathematical Sciences (DIISM), Università Politecnica delle Marche, Ancona, Italy

Abstract

In this study, it is aimed to design an efficient and sustainable solar tunnel dryer to be used in drying process of sewage sludge. In the first step of this study, heat and flow structure of three tunnel dryers including rectangular tunnel (RSTD), quonset tunnel (QSTD) and quonset tunnel with fins (QSTD/F) have been numerically surveyed to determine the effective design. Based on CFD results, quonset-type tunnel designs have been fabricated, experimentally analyzed and compared with numerical findings. In this work, different from previous studies on quonset-type solar-thermal systems, top surface of Quonset geometry was made from sheet metal as an absorber to enhance heat transfer area. The drying tests have been performed in different months of the year (June and January) by applying two different air velocities to evaluate the performance of tunnel dryers at various climatic conditions. Integrating fins to the quonset tunnel had considerable positive effects on both thermal and drying performances. According to the experimental findings, specific moisture extraction rate (SMER) value was attained on June and January in the range of 0.50e0.89 and 0.39e0.65 kg/kWh, respectively. The results indicated the successfulness of quonset solar tunnel dryer design in the dehumidification process of sewage sludge.

Keywords: Quonset, solar tunnel dryer, sewage sludge, solar thermal, solar drying.

Nomenclature	
A_{SD}	area (m^2)
COP	Coefficient of performance
c_p	specific heat capacity of air (kJ/kgK)
D_{hd}	hydraulic diameter (m)
DR	drying rate (g water/g dry matter min)
E_{fn}	overall consumed electrical energy (kJ)
EE	energy efficiency of the drying system (%)
G_b	generation of turbulence kinetic energy due to buoyancy (m^2/s^2)
G_k	generation of turbulence kinetic energy due to the mean velocity gradients (m^2/s^2)
h_{fg}	latent heat (kJ/kg)
I	solar radiation (W/m^2)
k	thermal conductivity (W/mK)
$\dot{m}$	mass flow rate (kg/s)
MC	moisture content (g water/g dry matter)
M_d	final dry weight (g)
M_i	initial wet weight (g)
M_m	removed water (kg)
Nu	Nusselt number
QSTD	Quonset solar tunnel dryer
QSTD/F	Quonset solar tunnel dryer with fins
Q_r	energy for the moisture removal (kJ)
$\dot{Q}_{uf}$	useful heat rate (W)
Re	Reynolds number
RSTD	Rectangular solar tunnel dryer
SEC	specific energy consumption (kWh/kg)
$SMER$	specific moisture extraction rate (kg/kWh)
T	temperature (K)
V	air velocity (m/s)
$\vec{v}$	overall velocity vector (m/s)
$\mathrm{w}_1, \mathrm{w}_2, \mathrm{w}_\mathrm{n}$	the uncertainties in the independent variables

W_{fn}	fan power (W)
W_R	Total uncertainty (%)
X_t	moisture content at time "t" (g water/g dry matter)
X_{t+dt}	moisture content at time "t+dt" (g water/g dry matter)
Greek letters	
α	absorptivity
α_ε	inverse effective Prandtl numbers for ε
α_k	inverse effective Prandtl numbers for k
λ	heat transfer coefficient (W/m^{2}K)
μ	dynamic viscosity of air (Pa.s)
ρ	density of air (kg/m^3)
τ	transmissivity
ω	specific humidity (g/g)
Subscripts	
in	inlet
out	outlet
a	air

1. Introduction

Supplying continuous and inexpensive energy resources is an important issue for countries that directly affect industrial and economic growth. Decreasing fossil reserves, environmental pollution and considering crude oil prices, renewable energy sources like solar energy has become an important matter of concern over the past decades [1-2]. Different studies were performed with the aim of analyzing environmental problems related to the conventional energy sources and the benefits of using clean energy systems. Also, a number of researches have been numerically and experimentally investigated renewable energy harvesting methods from different aspects of view. Investigating various studies showed that solar energy as a widely accessible clean and sustainable energy source can be used to obtain sustainable energy systems [3]. Utilizing efficient and innovative modifications, increasing the overall performance of renewable energy based systems, and combination with other energy systems are some of the top priority of available researches in the field of solar energy [4]. There is a remarkable attention to design innovative, cost-effective, simple structured and efficient solar-thermal energy systems with capability of absorbing high amount of solar energy [5]. Different types of solar thermal collectors were discussed in a study by Kalogirou [6]. Investigations on active solar energy systems indicates that integration of solar energy based systems can reduce the heating and cooling loads [7-9]. In addition, solar energy could be utilized with the aim of decreasing energy consumption in drying procedure which is an energy intensive process. Various types of direct and indirect solar-assisted drying systems are extensively investigated by different researchers all over the world [10]. Combining solar collectors with different drying systems could enhance the overall performance of the dryer. In a study performed by Ceylan and Gürel [11], a solar assisted a fluidized bed drying system combined with a heat pump with the aim of improving the efficiency of the system. In another study, Singh et al [12] indirect-expansion solar-infrared combined with a heat pump dryer to be utilized in drying agricultural crops. Also, Veeramanipriya, and Umayal Sundari [13] developed a hybrid photovoltaic thermal solar drying system with the purpose of capturing thermal energy and increasing the overall performance of the system.

Treatment of municipal sewage sludge is an important issue especially in big cities. In this context, sewage sludge can be dried by different drying methods and utilized in various applications that can decrease negative effects of direct disposal of sludge. Roof solar drying method was investigated by Wang et al. [14] in order to drying sewage sludge by using a sandwich-like chamber bed system. A combined system was designed by Di Fraia et al. [15] to use both solar energy and biogas as two different heat sources to be utilized for sewage sludge drying. In another work, a convex-type absorber was designed and manufactured by Tuncer et al. [16] for drying municipal sewage sludge. In a similar research numerical modeling method was used to analyze heat and moisture transfer of sewage sludge over drying process [17]. In another study, energy demand and drying behavior of a pilot-scale microwave system for sludge drying was investigated. In addition, drying rate, exposure time, and specific energy consumption were calculated to evaluate the performance of the dryer [18].

Solar tunnel drying systems have recently received remarkable consideration among community of researcher and engineers. Mewa et al. [19] conducted an experimental work to evaluate beef drying kinetics by using a solar tunnel dryer. Over the test time, different parameters were monitored and considered in calculations such as ambient humidity and temperature, air flow rate and solar radiation. Karthikeyan et al. [20] studied the drying kinetics of curcuma longa in a mixed mode forced convection utilizing solar tunnel drying system. Also, exergy analysis was performed using the obtained data from the experiments to evaluate the developed solar tunnel dryer. In another research, direct and indirect solar dryers were developed and their performance was evaluated in drying sewage sludge [21]. Also, a modified type of parabolic solar tunnel dryer was used with the aim of drying Andrographis paniculata [22]. In addition, solar tunnel applications have been performed in order to drying different agricultural products including potato chips, peppermint plants, ghost chilli pepper and mint [23-26].

Computational fluid dynamics (CFD) has been known as a numerical method used for simulating different energy systems which is widely utilized by different researchers. In the open literature, there are many scientific works on different solar energy-based systems like solar air heaters performed by using CFD as valuable method for evaluating the performance of the systems before manufacturing them [27-28]. Raj et al. [29] utilized CFD modeling with the aim of analyzing macro-encapsulated latent heat storage technique in a solar heating system. In other study, an artificially roughened solar air heater was simulated to determine the effect of various baffle modifications on the efficiency [30].

Drying sewage sludge is an important issue that has been studied by some researchers. The main purpose of dehumidifying sewage sludge is utilizing them in various applications. In this work, it is attempted to design an efficient and sustainable solar tunnel drying system to be used in drying process of sewage sludge. In this context, three various solar tunnel drying systems including rectangular tunnel (RSTD), quonset tunnel (QSTD) and quonset tunnel with fins (QSTD/F) have been investigated with the aim of improving heat transfer. The major purpose of this work is determining the most suitable configuration for solar tunnel dryer. Also, it was aimed to specify the performance of solar energy-based tunnel dryers in drying process of sewage sludge. In this manner, heat and flow structure of three tunnel dryers have been numerically surveyed to select the effective design. In addition, effective tunnel designs have been fabricated, experimentally analyzed and compared with simulation results. In Fig. 1, main steps of the present research is displayed and explained briefly.

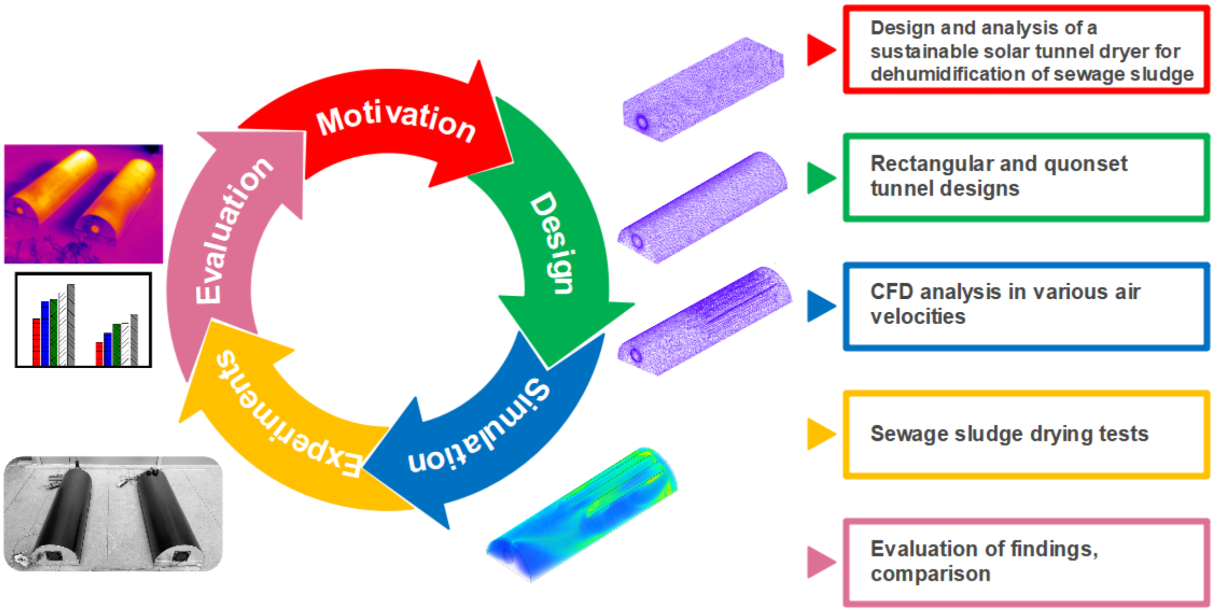

Fig. 1. Main steps of the present study

2. CFD simulation

Computational fluid dynamics is an important tool with outstanding accuracy and flexibility used in different investigations, which involves the use of the basic laws of energy, governing equations and modeling a physical problem. CFD simulation is a very useful method to analyze the pressure, velocity, temperature, and density of analyzed zone. This technique is widely used by researchers to compare with experimental work and to closely monitor the flow structure and temperature distribution of the utilized fluid. This methodology, is used especially for the purpose of revealing the structure of flow field, which can be very useful because flow imaging is a very difficult process and sometimes just impossible for some experimental works. In this section, three different tunnel dryers have been analyzed to determine the most suitable geometry of tunnel dryer. In this regard, rectangular tunnel (RSTD), quonset tunnel (QSTD) and quonset tunnel with fins (QSTD/F) have been generated and analyzed. In Fig. 2, geometry and boundary conditions for analyzed solar tunnel dryers are given. Inlet, outlet, solar radiation and fins placement are clearly displayed in Fig.

2. Mesh generation is another important step in the numerical analysis. In Fig. 3, the generated mesh configurations of test tunnels have been provided for all geometries. Various mesh types, configurations and modifications have been performed to achieve appropriate mesh structure for each geometry and consequently obtaining high accuracy in the numerical outcomes. As shown in the Fig. 3, triangle mesh and curvature mode were utilized with 1.2 growth rate. The skewness quality factor as a significant parameter was evaluated in mesh generation process. For generated meshes, average and highest skewness values in this case study varied between 0.23-0.26 and 0.80-0.84, respectively. Moreover, mesh elements number of the models in RSTD, QSTD and QSTD/F dryers were obtained as 1430000, 1450000 and 1490000, respectively.

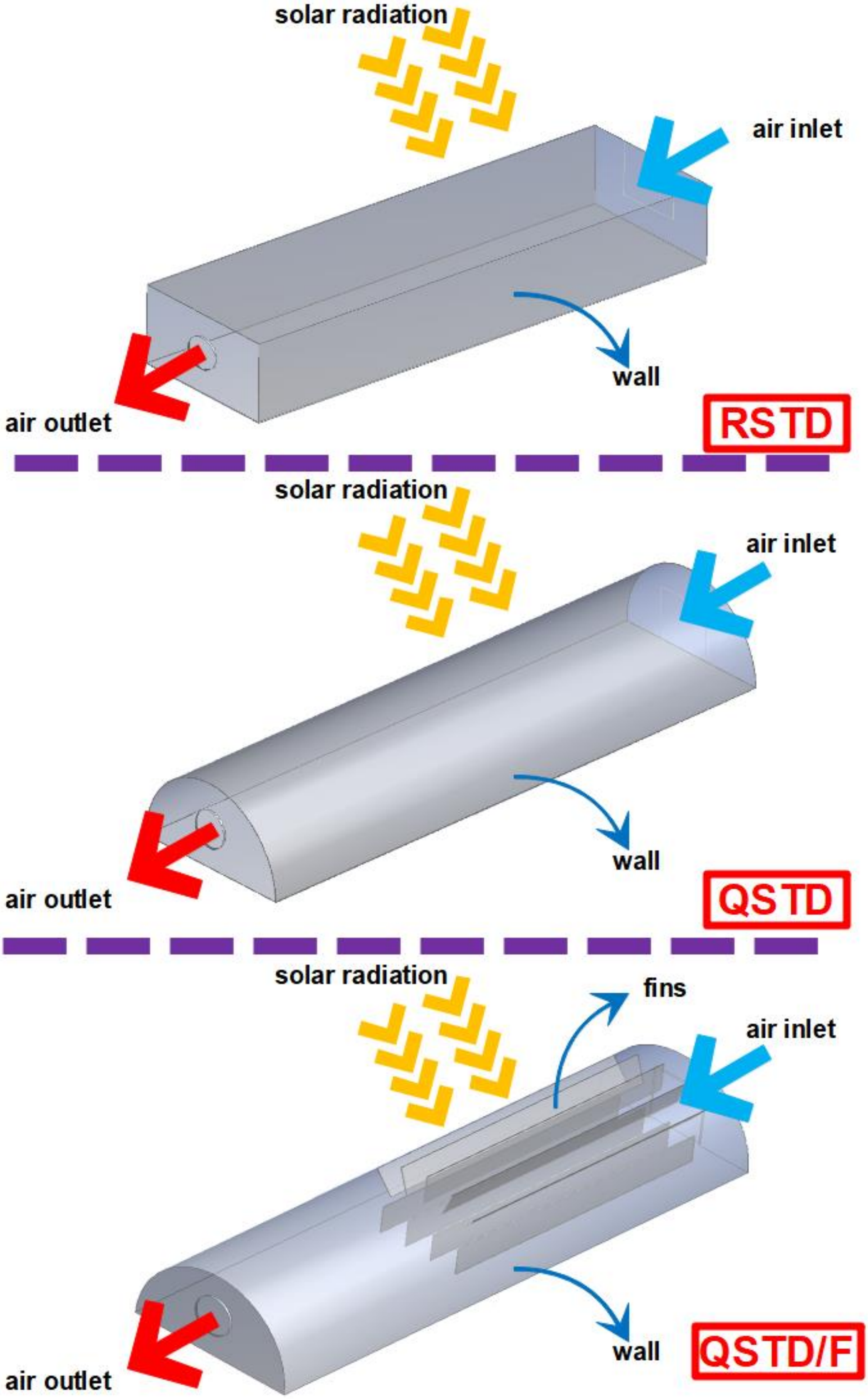

148

149 **Fig. 2.** Geometry and boundary condition for solar tunnel dryers

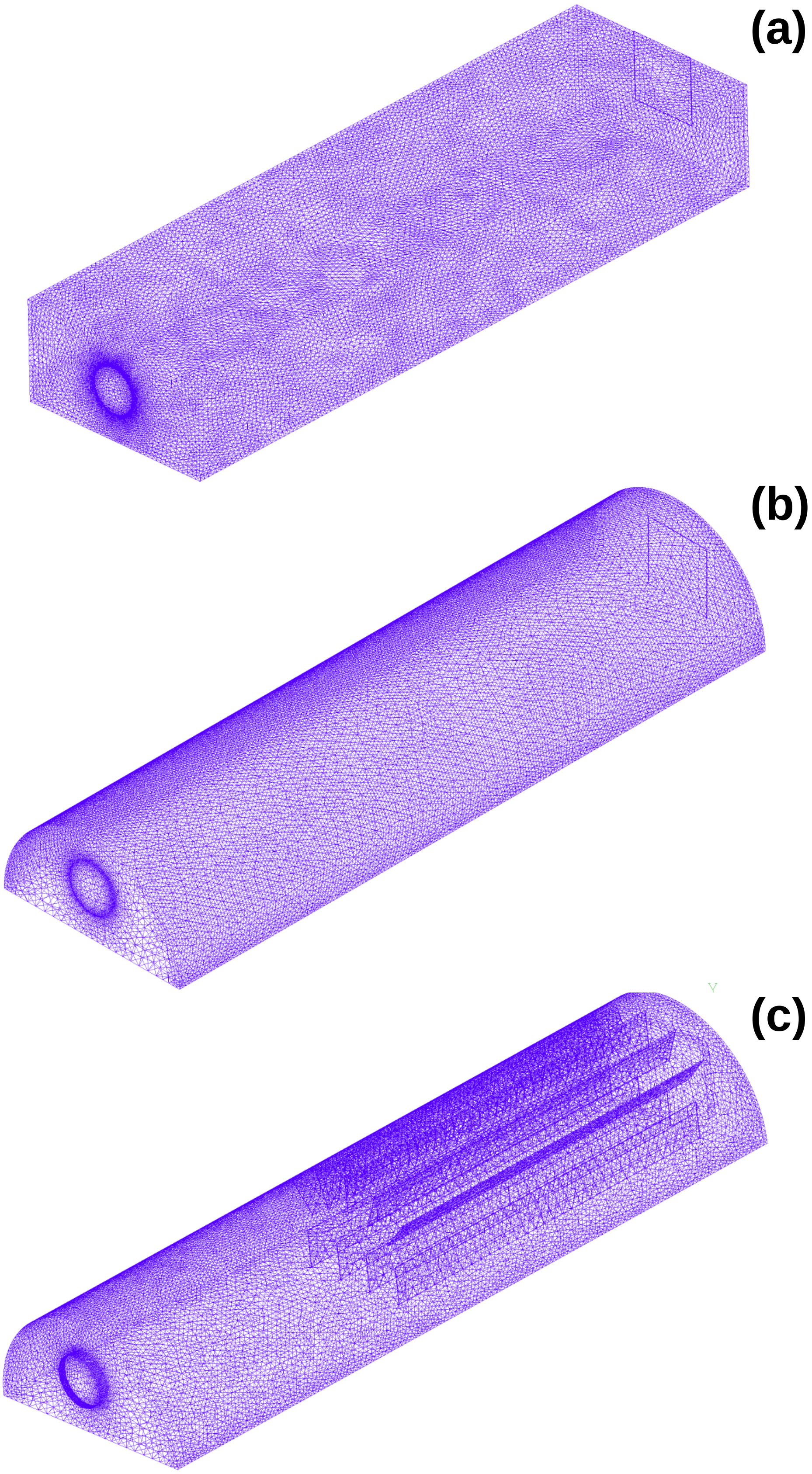

Fig. 3. The generated mesh for three tunnel dryers

The main aims of CFD analysis in this study are determining the most suitable geometry for tunnel dryer and specifying the effect of integrating fins. In this regard a steady-state model has been utilized in CFD simulation part. In this research, the effect of air specific humidity is neglected and the thermal performance of the system is analyzed. In other words, the potential of the designed tunnel dryers in heating flowing air is investigated. In this study, dried sample is sewage sludge and unlike agricultural products high air temperature is intended to reduce drying time. In accordance with experimental conditions, boundary values have been defined to apply in the derivation of energy, continuity and momentum equations. Defined problem was assumed to be a three-dimensional geometry under a turbulent flow. Governing equations are given as:

Mass conservation:

$$\nabla.(\rho.\vec{v}) = 0 \tag{1}$$

Momentum balance:

$$\nabla.(\rho.\vec{v}.\vec{v}) = -\nabla p + \nabla.(\mu\left[(\nabla\vec{v} + \nabla\vec{v}^T) - \frac{2}{3}\nabla.\vec{v}I\right]) \tag{2}$$

Energy conservation balance:

$$\nabla.\left(\vec{V}(\rho E + p)\right) = \nabla.k_{eff}\nabla T - h\vec{J} + (\mu\left[(\nabla\vec{v} + \nabla\vec{v}^T) - \frac{2}{3}\nabla.\vec{v}I\right].\vec{v}) \tag{3}$$

In the CFD method, $\mathrm{k}-\varepsilon$ viscous model is known as one of the most useful models which is appropriate for turbulence flow. Basically, two transport equations are employed in solution of this method, which are known as “k” for turbulent kinetic energy and “ε”, for the rate of dissipation of kinetic energy. In this work, $\mathrm{k}-\varepsilon$ RNG model has been used in solution which can be expressed by following equations [31]:

$$\frac{\partial}{\partial t}(\rho k) + \frac{\partial}{\partial x_i}(\rho k u_i) = \frac{\partial}{\partial x_j}\left(\alpha_k \mu_{eff}\frac{\partial k}{\partial x_j}\right) + G_k + G_b - \rho\varepsilon - Y_M + S_k \tag{4}$$

$$\frac{\partial}{\partial t}(\rho\varepsilon) + \frac{\partial}{\partial x_i}(\rho\varepsilon u_i) = \frac{\partial}{\partial x_i}\left(\alpha_\varepsilon \mu_{eff}\frac{\partial \varepsilon}{\partial x_j}\right) + C_{1\varepsilon}\frac{\varepsilon}{k}(G_k + C_{3\varepsilon}G_b) - C_{2\varepsilon}\rho\frac{\varepsilon^2}{k} - R_\varepsilon + S_\varepsilon \tag{5}$$

here, S_k and S_ε are source terms. Y_M shows contribution of the fluctuating dilatation in compressible turbulence to the overall dissipation Also, $C_{1\varepsilon}$, $C_{2\varepsilon}$ and $C_{3\varepsilon}$ are model constants.

3. Material and Method

3.1. System design

In the experimental analysis part of this work, tunnel dryers with two different geometries have been manufactured for sustainable solar assisted dryers by considering CFD simulation results. The obtained results in numerical analysis part and analyzing the presented studies in the literature indicated the superiority of quonset geometry in comparison to rectangular geometry [32-35]. In this regard, two different quonset type solar tunnel dryers have been fabricated to be tested experimentally. The first one was named as quonset type solar tunnel dryer (QSTD). In the second one, 5 fins placed on absorber surface and 4 fins on the dryer floor and was named as quonset type solar tunnel dryer with fins (QSTD/F). Both dryers' bottom side has a base size of 1000x300 mm. The radius of quonset absorber is 150 mm. The fins added to QSTD/F dryer placed 50 mm after the fan inlet and their dimensions are as 50x500 mm. In Fig. 4, the internal details of the dryers are shown.

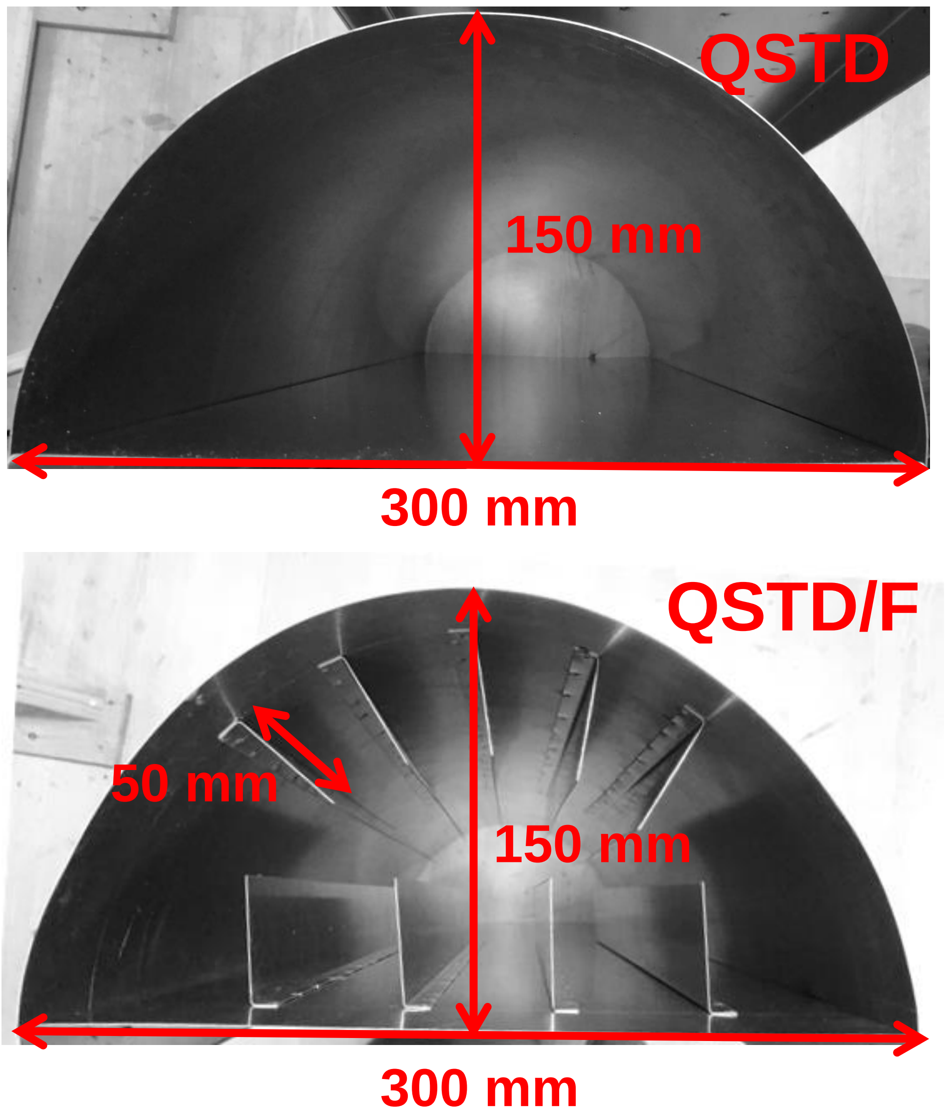

Fig. 4. Internal details of quonset solar dryers

3.2. Experimental setup

The experimental setup was fabricated considering the numerically obtained results. 1 mm thick metal sheet was used in the manufacturing stage of the dryers. The base plate, quonset structure and fins are all made of the same material. 50 mm thick carbon reinforced expanded polystyrene thermal insulation material was placed on the bottom of both dryers. In addition, 20 mm thick extruded polystyrene thermal insulation material was used in the air inlets and outlets. In the experiments, 40 W alternating current fans were used and suitable dimmer switches were added to control air velocity in the system. A schematic diagram and a photograph of the experimental setups are shown in Fig. 5.

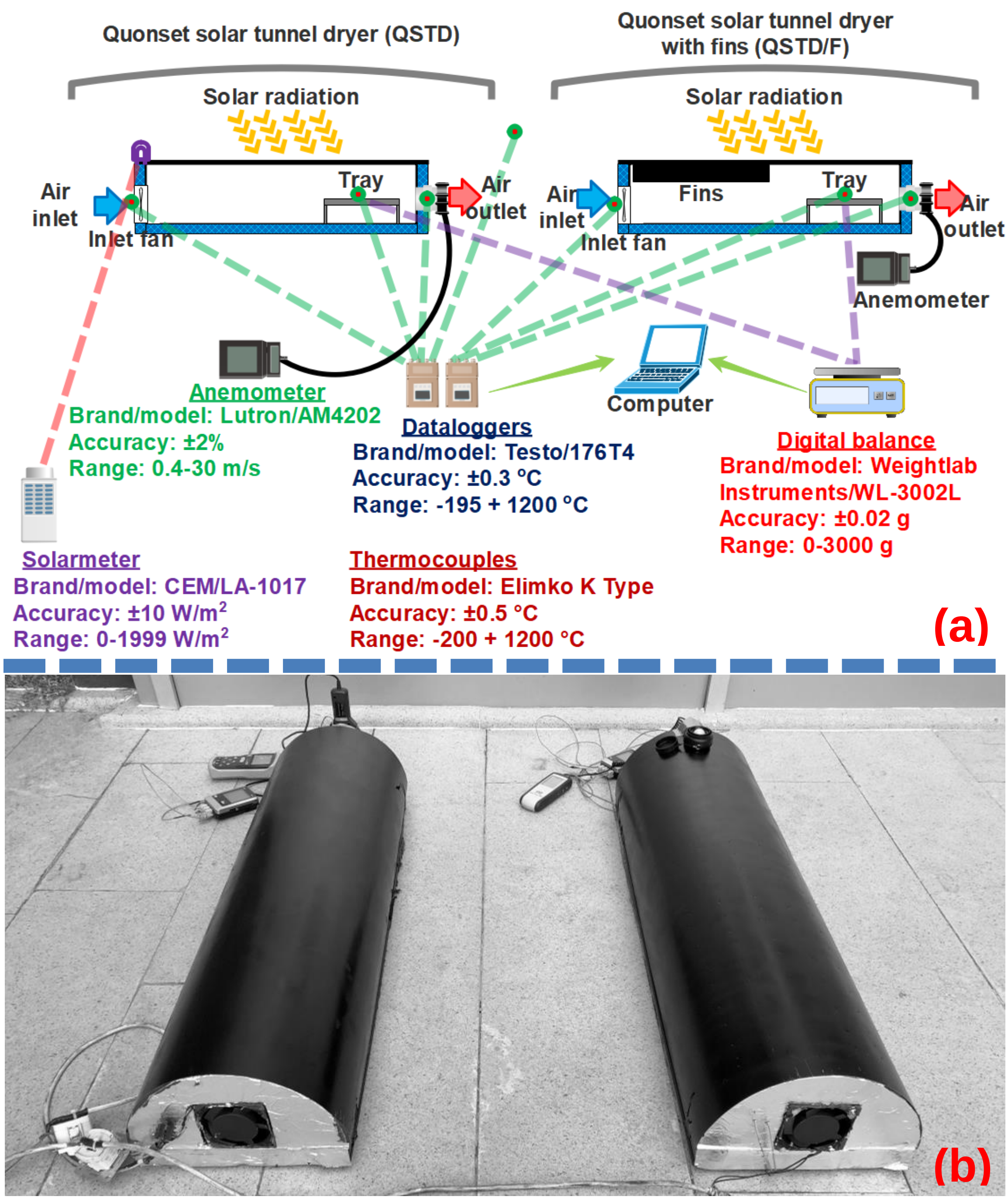

Fig. 5. Experimental setup of tunnel dryers; a) Schematic diagram, (b) Photograph

3.3. Experimental procedure

In this study, both QSTD and QSTD/F systems were tested simultaneously to analyze their performance and examine the effect of adding fins to quonset type dryer. The experiments were carried out on June and January on four different days by applying two different air velocities to compare the performance of tunnel dryers at various climatic conditions. This experimental process could provide a general view about the performance of the manufactured tunnel dryers.In the experiments, air velocities were set to 3 m/s (Exp. 1) and 2 m/s (Exp. 2). These air velocities correspond to 0.014 kg/s and 0.009 kg/s air mass flow, respectively. Air flow rate is an important factor in drying applications. It should be indicated that air flow above the drying sample has two different duties containing cooling effect and conveying evaporated moisture from drying sample surface. It is clear that high air flow rate leads to increases in cooling impact, so the evaporation rate reduces. Consequently, the optimum flow rate is needed to achieve a balance among sample cooling and removal of evaporated moisture. In this work, the experiments have been conducted at two different air flow rates including 0.014 kg/s and 0.009 kg/s regarding to similar drying application in the literature [11,36, 37]. Before starting the experiments, both systems were kept covered in ambient conditions and turned to the south. Moreover, the fans were started to run 20 minutes before starting experiments.

Sewage sludge samples with the density of 1370 kg/m^3 were placed in both systems as 100 grams in per tray. The tray is located 80 mm above from the baseplate and the tray dimensions are 250x250 mm. The tray is positioned 100 mm away from the air outlet. The purpose of this placement is to make maximum use of the heated air. Temperature measurements were performed by K-type thermocouples. Temperature values were measured every 5 seconds and recorded with the help of data loggers. Air velocity, solar radiation and mass flow variations were measured at 20 minutes intervals by using anemometer, solar meter and digital balance, respectively. Details of measuring equipment can be seen in Fig. 5. Used sewage sludge drying sample had a premier moisture content of 4.50±0.30 g water/g dry matter. The performance tests begun at 09:00 AM and ended when the difference among two weight measuring was lower than 1%.

4. Theoretical calculations

In this part, the used expressions in investigating quonset type solar tunnel dryers are given. Mass conversation of air and moisture could be expressed by using Eq. (6) and Eq. (7), respectively:

$$\sum \dot{m}_{in,a} = \sum \dot{m}_{out,a} \tag{6}$$

$$\sum\left(\dot{m}_{in,a}.\omega_{in,a} + \dot{m}_m\right) = \sum \dot{m}_{out,a}.\omega_{out,a} \tag{7}$$

The energy balance in the quoset type dryer could be defined as:

$$\dot{Q}_{in} - \dot{Q}_{loss} = \dot{m}_a\left(h_{out,a} - h_{in,a}\right) \tag{8}$$

The input thermal energy to the solar dryer can be obtained by using Eq. (9):

$$\dot{Q}_{in} = \alpha.\tau.I.A_{SD} \tag{9}$$

The gained useful thermal energy in the solar drying system could be found as:

$$\dot{Q}_{uf} = \dot{m}_a.c_p.\left(T_{out,a} - T_{in,a}\right) \tag{10}$$

Coefficient of performance (COP) is a substantial metric in investigating energy applications. COP can be defined as the ratio of overall gained thermal energy to total used electrical power. In this study, the overall used electrical power refers to utilized fan power. COP could be calculated by utilizing Eq. (11):

$$COP = \frac{V_a.\rho.c_p.(T_{out,a} - T_{in,a})}{W_{fn}} \tag{11}$$

Reynolds and Nusselt numbers are important dimensionless metrics that are utilized in investigating thermal and flow behavior. Reynolds number could be achieved by using Eq. (12) [38]:

$$Re = \frac{\rho.V.D_{hd}}{\mu} \tag{12}$$

Nusselt number can be found as:

$$Nu = \frac{\lambda.D_{hd}}{k} \tag{13}$$

Specific moisture extraction rate (SMER) and specific energy consumption (SEC) are crucial parameters that could be used for analyzing the effectiveness of dryers. SMER can be defined as the amount of moisture extracted per used electrical energy and can be calculated as:

$$SMER = M_m/E_{fn} \tag{14}$$

Energy efficiency of the dryer (EE) is a crucial metric to investigate the effectiveness of the developed and analyzed drying system. It could be achieved by dividing the amount of needed thermal energy to extract moisture from the sample to required electrical energy. EE could be obtained as:

$$EE = Q_r/E_{fn} \tag{15}$$

The thermal energy used to extract moisture from municipal sewage sludge sample could be obtained by using Eq. (16) [16]:

$$Q_r = h_{fg} \cdot M_m \tag{16}$$

Moisture content on dry basis and drying rate can be found with the help of the following expressions [39]:

$$MC = \left(\frac{M_i - M_d}{M_d}\right)100 \tag{17}$$

$$DR = \frac{X_{t+dt} - X_t}{dt} \tag{18}$$

General expression for experimental uncertainty can be expressed as [40-41]:

$$W_R = \left[\left(\frac{\partial R}{\partial x_1}w_1\right)^2 + \left(\frac{\partial R}{\partial x_2}w_2\right)^2 + \cdots + \left(\frac{\partial R}{\partial x_n}w_n\right)^2\right]^{1/2} \tag{19}$$

5. Results and Discussion

5.1. CFD Results

In this section, the obtained numerical results for different designs and operating conditions are given and explained. CFD analysis have been done considering average conditions of June and January. In this part, temperature and velocity contours related to June condition are presented. Also, in the experimental results section, numerically obtained outlet temperatures related to June and January are presented and compared with experimentally attained outlet temperatures. In Fig. 6, velocity contours of various solar tunnel dryers are presented for two different air velocities. Considering obtained contours, the highest air velocity is seen in the center of the tunnel, and as expected the velocity decreases as it approaches the walls, where velocity value is low as a result of friction. Analyzing velocity distribution in different tunnel dryers indicated that using quonset type tunnel can led to obtain more homogeneous flow inside the dryer. In other words, in rectangular tunnel air flows over the middle part of the tunnel and quit the system. However, in quonset type tunnel more homogenous velocity distribution is available and air flows over all surface that can attain more thermal energy.

In Fig. 7, temperature contours for analyzed solar tunnel dryers have been presented. The effect of air velocity is clearly observed in the obtained temperature contours for different tunnel dryers. The effect of increasing velocity from 2 m/s to 3 m/s on air temperature on reducing the temperature obviously can be seen especially in the boundaries and near walls. In addition, positive impact of using fins in designed QSTD/F system indicates that this type of fins' use can be considered in solar systems to improve thermal characteristics of the solar tunnel dryers.

The results obtained from volume rendering method are considered to be one of the most important figures achieved from modeling. The three-dimensional figures obtained by this methodology provide a better perspective for understanding the velocity distribution, flow structure and temperature distribution of the fluid. As it can be clearly shown in Fig. 8a, the temperature level is higher in the areas close to the fins and the heat is transferred from the wall and the fins to the fluid. In addition, velocity volume rendering is given in Fig. 8b. As shown in this figure, the highest velocity values are clearly obtained from the simulation in the entrance (inlet) and exit areas.

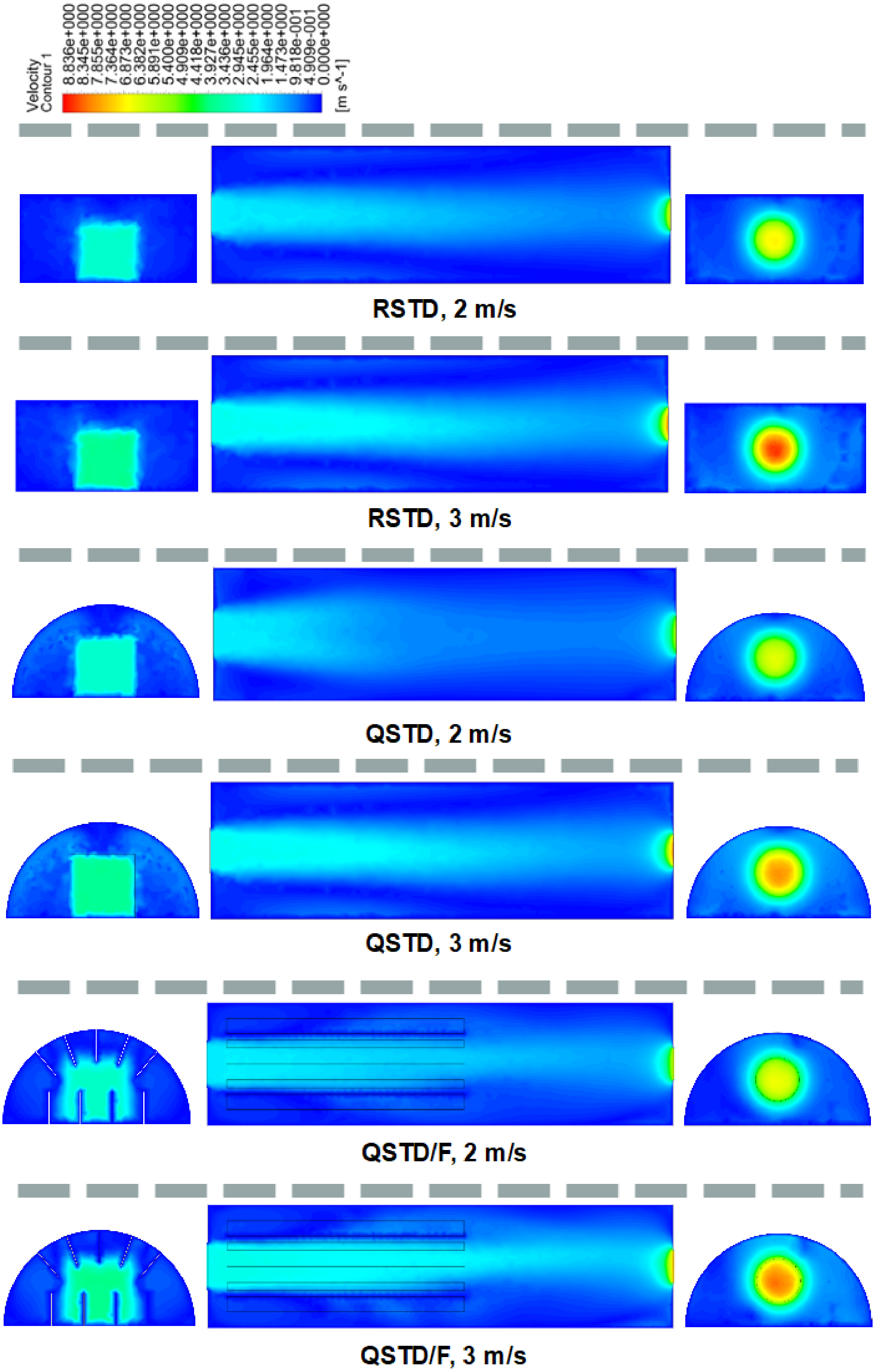
Velocity
Contour 1
8.836e+000
8.345e+000
7.855e+000
7.364e+000
6.873e+000
6.382e+000
5.891e+000
5.400e+000
4.909e+000
4.418e+000
3.927e+000
3.436e+000
2.945e+000
2.455e+000
1.964e+000
1.473e+000
9.818e-001
4.909e-001
0.000e+000
[m s^-1]
RSTD, 2 m/s
RSTD, 3 m/s
QSTD, 2 m/s
QSTD, 3 m/s
QSTD/F, 2 m/s
QSTD/F, 3 m/s

Fig. 6. Velocity contours for solar tunnel dryers

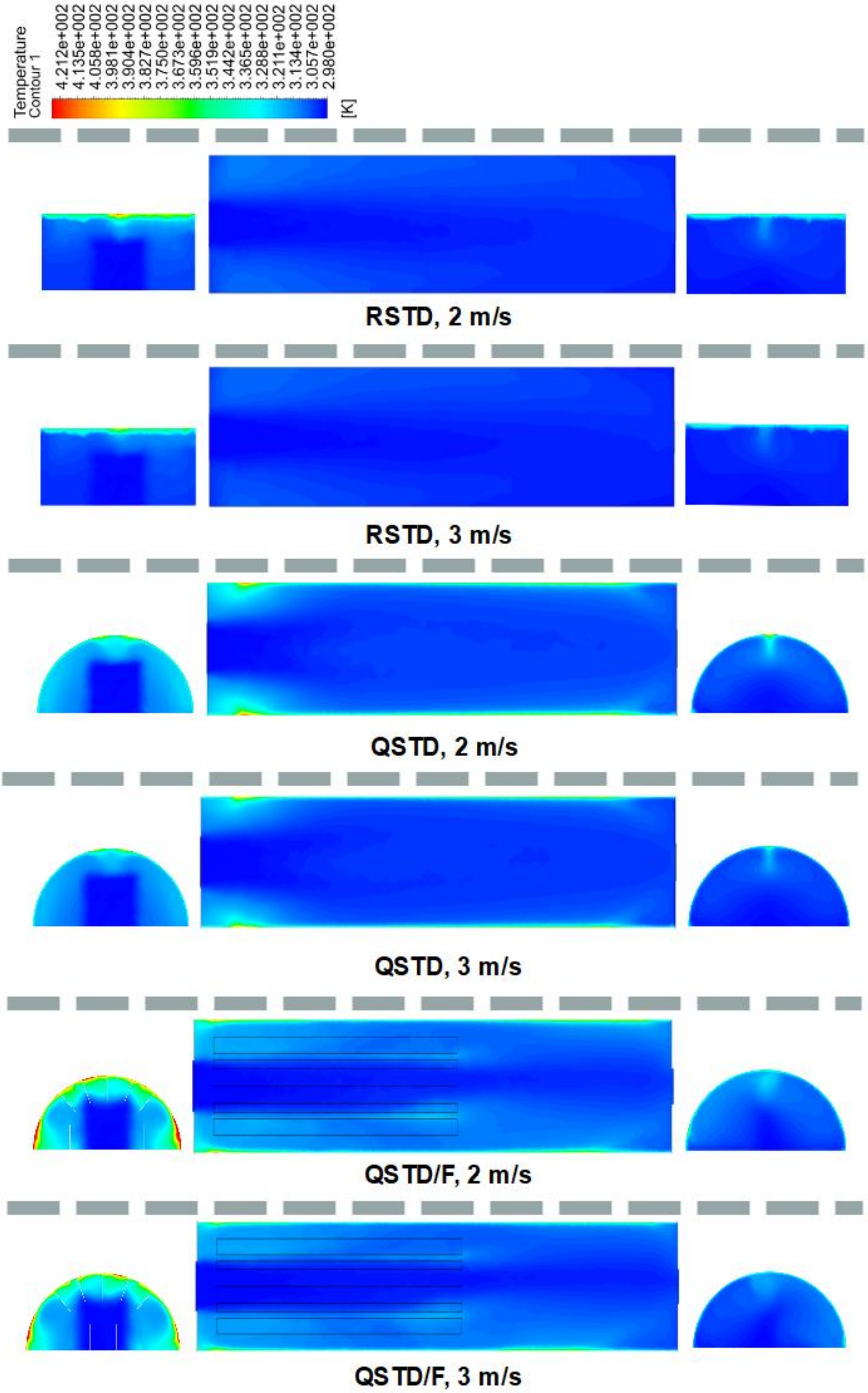

Fig. 7. Temperature contours for solar tunnel dryers

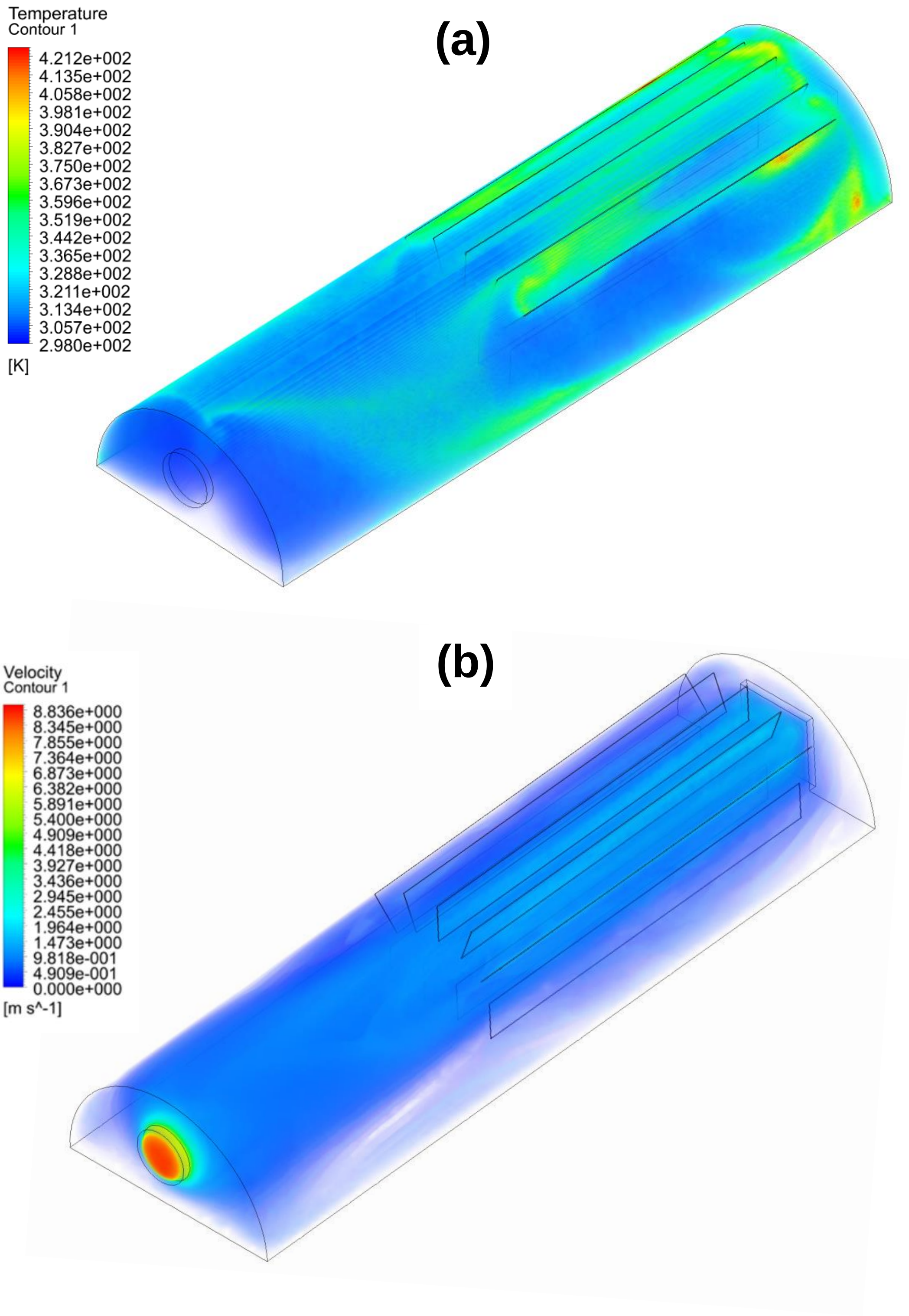

Fig. 8. Volume rendering images of QSTD/F at 2 m/s air velocity; a) temperature, b) velocity

5.2. Experimental results

The experiments have been carried out at two different air velocities as 2 and 3 m/s. In Fig. 9, time-dependent solar radiation and change of ambient temperature in the experiments done on June and January are given. Since the experiments have been performed on consecutive days on June and January, the values are very close to each other. This issue allows to make reasonable comparisons between obtained results. In the experiments 1, 2, 3 and 4 the average solar radiation values were measured as 836, 858, 734 and 726 W/m^2, respectively. Also, average ambient temperature values were observed as 25.6°C, 26.2°C, 14.16°C and 13.87°C respectively. Maximum solar radiation values for Exp. 1, Exp. 2, Exp. 3 and Exp. 4 is 948, 953, 816 and 828 W/m^2, respectively.

The COP is generally used in thermal systems and is an important parameter for determining the system performance in solar-assisted energy systems. Briefly, the COP value can be defined as the ratio of the useful energy obtained to the consumed energy in the system. The electrical power value as consumed energy for the present system is very low. COP variation with the time is illustrated in Fig. 10. For the experiment 1, COP values were calculated as 4.88 and 4.25 for QSTD/F and QSTD in the experiment performed at 3 m/s air velocity. These values were calculated for the experiment 2 as 4.28 and 3.86 respectively. In the experiment 3, COP for QSTD/F and QSTD was achieved as 4.08 and 3.66, respectively. In addition, in the experiment 4, COP for QSTD/F and QSTD was attained as 3.45 and 3.11, respectively. In a work conducted by Güler et al. [36], a solar dryer was made utilizing a double-flow collector modified with iron mesh. In that study, the obtained COP values were attained in the range of 4.83-5.53. It can be state that, similar results were obtained when compared to the present study. The reason for the relatively higher COP values in the related study arose from harvesting more useful energy by using double-pass structure. In other study performed by Sözen et al. [42], COP value was achieved in the range of 3.10-3.87. Also, in another work different turbulator modifications were applied to a tubular solar collector [43] and average COP value was achieved as 3.80. By examining similar academic researches in the literature, it is revealed that, the COP values obtained in this research are in the agreement with other studies.

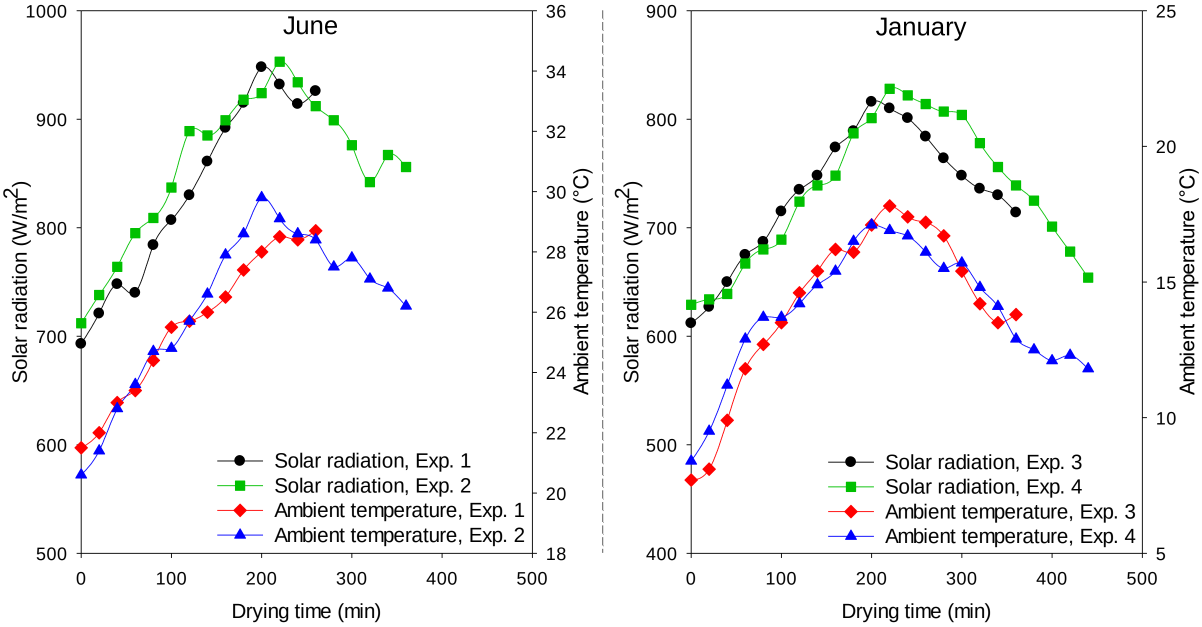

Fig. 9. Time dependent variation of solar radiation and ambient temperature values

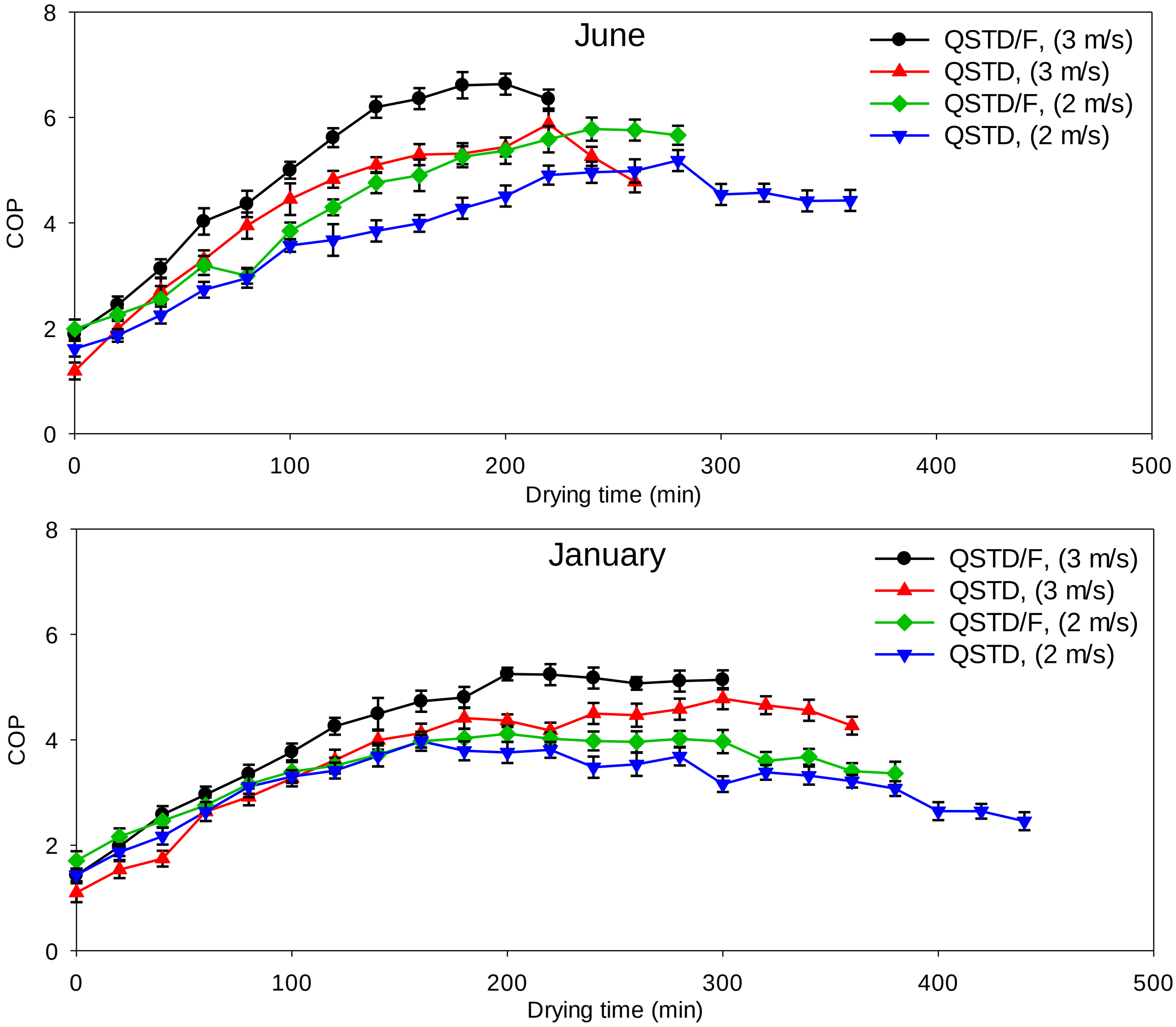

Fig. 10. Time dependent variation of COP values

The MC variation with respect to the test time is shown in Fig. 11. From the figure, it can be seen that, in the experiment performed at high air velocity on June, the modified quonset dryer could shorten the drying time by 40 minutes, and by 80 minutes at low air velocity. Also, in the experiments conducted on the winter condition (January) drying time was shortened as 60 and 60 minutes at high and low air velocities, respectively. Accordingly, it can be stated that, both the impacts of air velocity and the fin integration on drying performance of the system are quite significant. The shortest drying time was observed as 220 minutes in the experiment using the fin assisted quonset dryer on June. The influence of air velocity in solar assisted drying systems has been reported in similar available in the literature [44-47].

In Fig. 12, SMER change with time is shown. Average SMER values were calculated as 0.89 and 0.76 kg/kWh for QSTD/F and QSTD, respectively in the experiment performed at 3 m/s air velocity on June. For the experiments at the air velocity of 2 m/s on June, it was calculated as 0.55 kg/kWh and 0.50 kg/kWh, respectively. Also, average SMER values in the experiment performed at 3 m/s air velocity on January obtained as 0.65 and 0.54 kg/kWh for QSTD/F and QSTD, respectively. Moreover, average SMER values in the experiment conducted at 2 m/s air velocity on January obtained as 0.43 and 0.39 kg/kWh for QSTD/F and QSTD, respectively. As it was expected, the SMER values for both dryers at high air velocity are high. However, longitudinal fins added to QSTD/F caused a significant increase in SMER values.

Fig. 13 illustrates a comparison of the SMER values for solar-assisted drying systems in this work and related studies in the literature. As shown in the figure, in some presented studies more complex systems such as solar-assisted fluidized-bed [48], solar-assisted heat pump [49], photovoltaic-thermal [50] used in drying systems to achieve higher performance. At the same time, it was found that obtained results from present work is in harmony in terms of SMER values compared to similar solar assisted systems performed recently [1, 16, 42, 51-58].

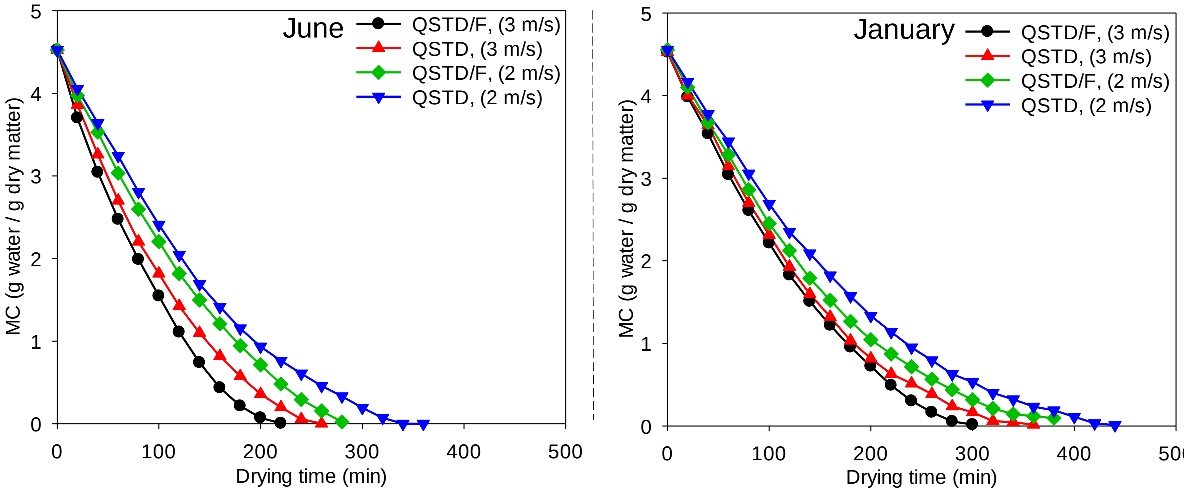

Fig. 11. Time dependent variation of MC values

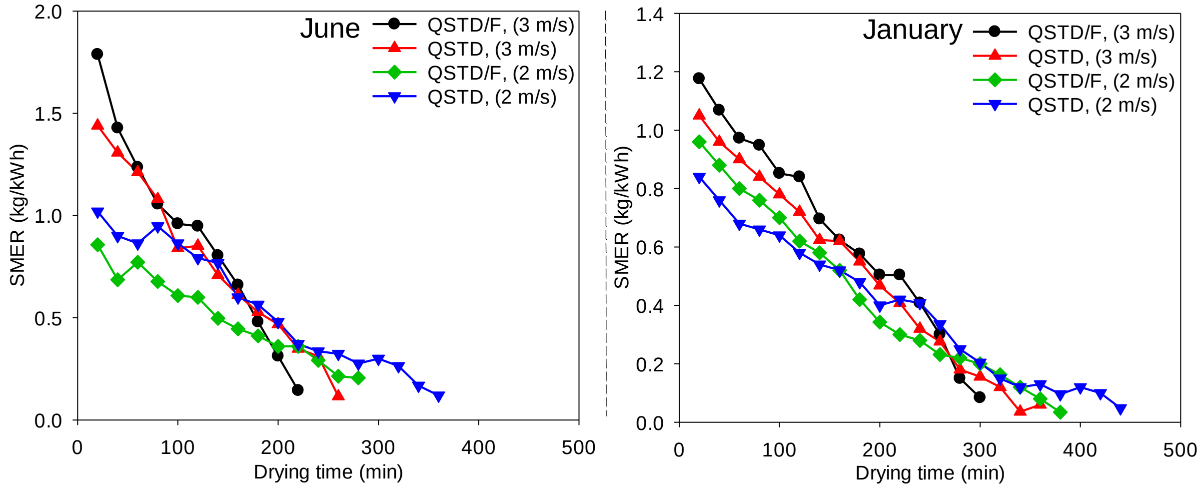

Fig. 12. Time dependent variation of SMER values

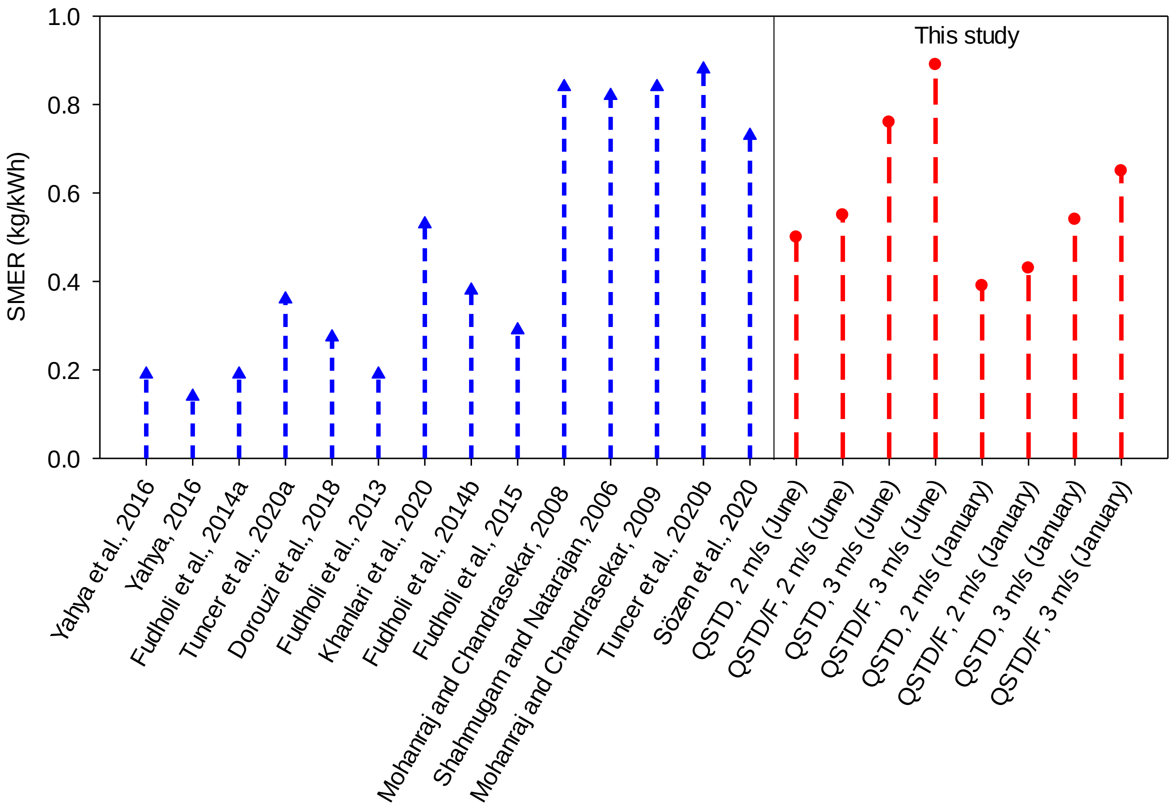

Fig. 13. Comparison of obtained SMER values with available studies about solar dryers in the literature

Fig. 14 gives the change of DR values with test time. Accordingly, for QSTD/F dryer average DR values were calculated as 0.0018, 0.0011, 0.0010 and 0.0006 g water/g dry matter min for experiment 1, 2, 3 and 4, respectively. DR values were found as 0.0013, 0.0007, 0.0006 and 0.0005 g water/g dry matter min for QSTD, for experiment 1, 2, 3 and 4, respectively. As seen in Fig. 14, reducing moisture content of sewage sludge sample over the time led to reduce in DR values. It can be expressed that the air mass flow rate has a significant influence on transferring water from sample surface and as a result drying process can be accelerated. It is better to state that agricultural products generally have certain moisture contents. In other words, moisture content of the same product does not significantly vary regionally. This fact makes it possible to determine initial moisture content and adjusting the drying system's set values. In this study, municipal sewage sludge has been dried as sample. Different parameters could affect the characteristics of sewage sludge sample. Therefore, sewage sludge samples provided from different treatment plants have not the same properties. Consequently, adjusting a drying system based on specification of a sewage sludge sample is not reasonable.

In the experiments done on June, average energy efficiency (EE) values of QSTD/F and QSTD dryers at 3 m/s air velocity were found as 44.32% and 37.53%, respectively. Also, for low air velocity (2 m/s), average EE values for QSTD/F and QSTD dryers are 40.93% and 36.23%, respectively. In the experiments performed on January, average EE values of QSTD/F and QSTD dryers at 3 m/s air velocity were attained as 32.42% and 27.02%, respectively. In addition, average EE values of QSTD/F and QSTD dryers at 2 m/s air velocity were achieved as 25.19% and 22.16%, respectively. As seen, EE values on January experiments are lower than that of the experiments done on June. It can be stated that some factors such as low solar radiation and low ambient temperature affected the performance of drying system negatively in winter. In a study on a solar-assisted waste sludge drying system, EE found in the range of 21-47% [16]. In a study where a solar-assisted system was used for drying agricultural products, these values were calculated in the range of 17-34% [59]. In these two mentioned studies, both air velocity and modifications increased EE values similar to the current research. Since waste sludge was selected as the product to be dried in this study, there is no concern about the product quality, which is important in agricultural products. For this reason, high air velocities can be preferred for efficient drying and high energy efficiency in solar assisted drying systems designed for drying waste sludge.

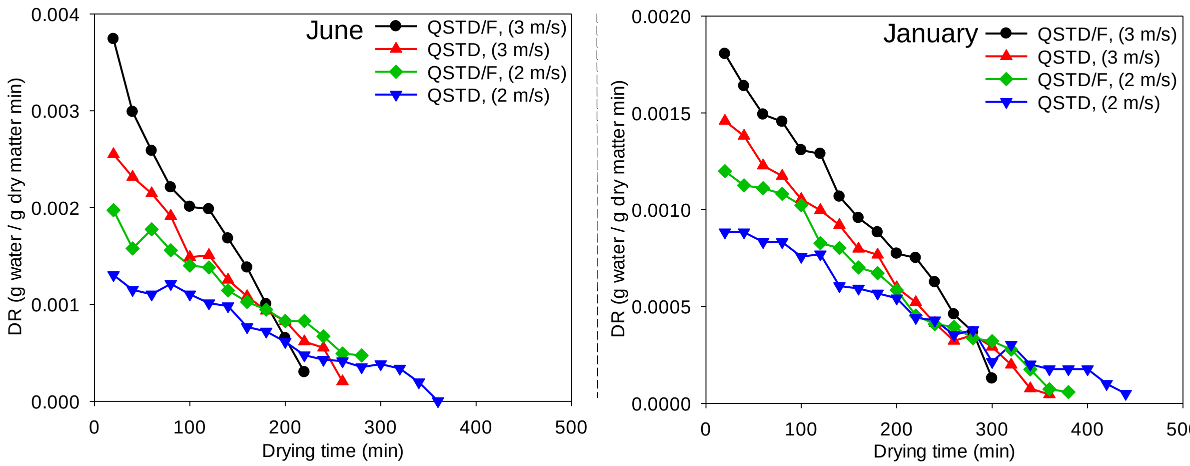

Fig. 14. Time dependent variation of DR values

Fig. 15 shows the numerical and experimental results of the outlet temperature values. From the figure, it can be seen that the outlet temperature of the rectangular dryer is very low compared to the other systems. For this reason, this model was not used in the experimental study and quonset form dryers were preferred. Experimental and numerical results for low air velocity on June conditions have deviations of 5.14% and 5.71% for QSTD/F and QSTD, respectively. Also, these values on June conditions are 6.5% and 7.42% respectively for high air velocity. Experimental and numerical findings for low air velocity on January conditions have deviations of 5.24% and 7.43% for QSTD/F and QSTD, respectively. In addition, these values on January conditions are 7.74% and 6.92% respectively for high air velocity. Fig. 16 shows a thermal camera image taken during the experiment 1. As it can be seen in Fig. 16, adding fins to the tunnel dryer led to obtain higher temperature in the absorber surface in comparison with unmodified one.

Table 1 represents the obtained experimental uncertainty values in the performance tests. The attained values for experimental uncertainties are in acceptable range when compared with literature studies [4, 11, 53].

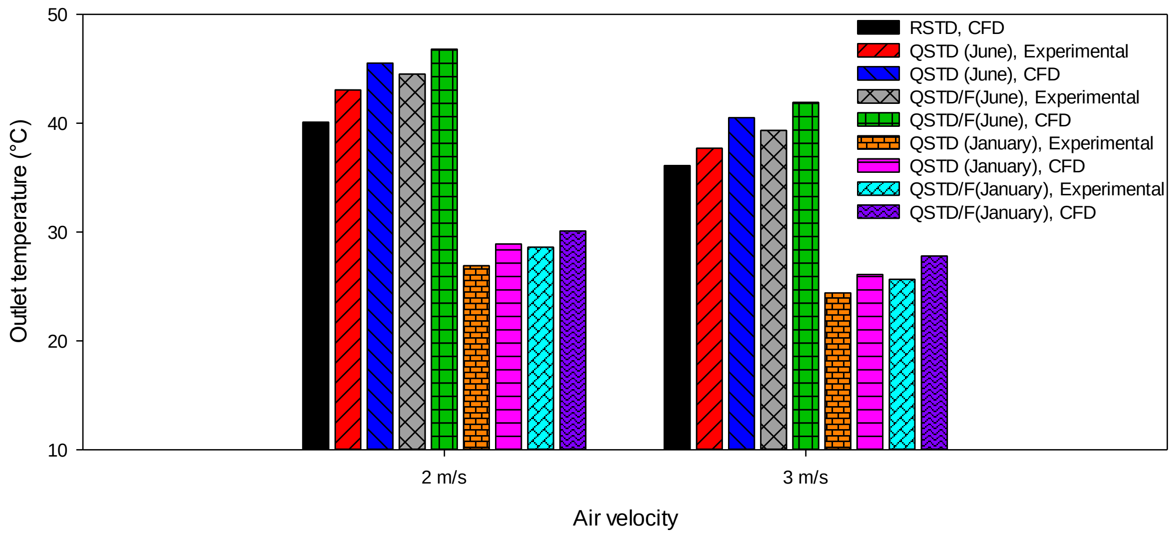

Fig. 15. Obtained numerical and experimental outlet temperature values

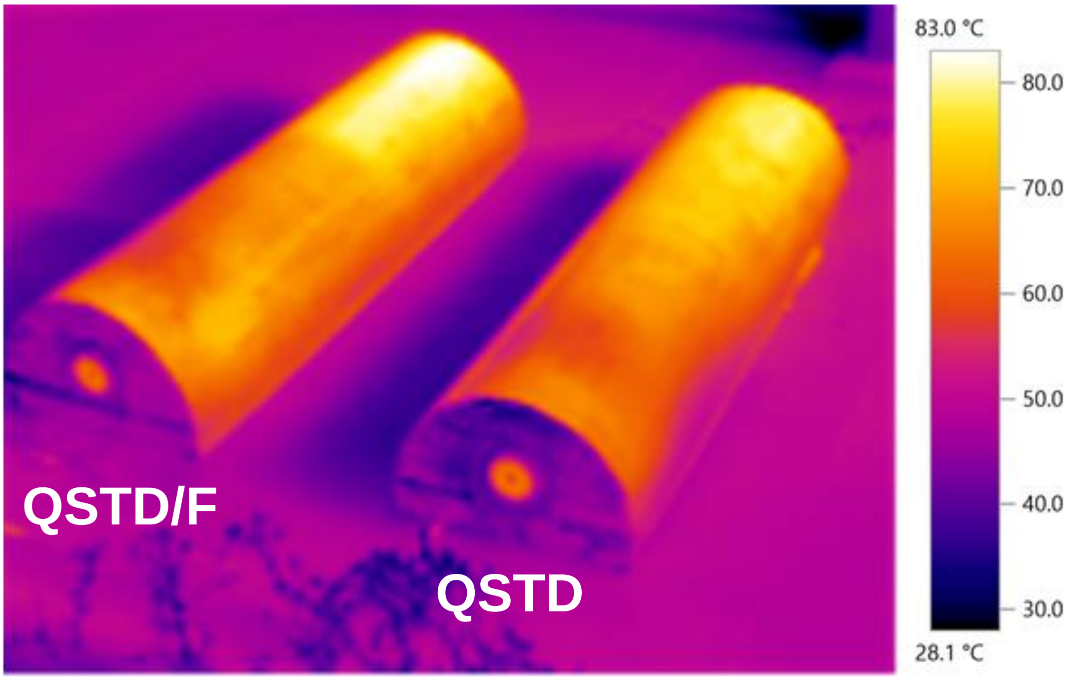

Fig. 16. Thermal camera view of the tested solar dryers

Table 1. The obtained experimental uncertainty values

Parameter	Unit	Uncertainty
Temperature	˚C	±0.64
Solar radiation	W/m^2	±16.68
Air velocity	m/s	±0.34
COP	-	±0.24

Tunnel dryers are widely utilized in different drying applications. In addition, solar energy assisted tunnel dryers are extensively analyzed by some researchers. Large scale tunnel dryers were developed and analyzed for different scenarios [60-62]. Analyzing available solar tunnel dryers exhibited high potential of this type dryers that could be utilized for drying various products. In some tunnel dryers, transparent cover has been utilized that can be affect the structure and durability of drying system negatively. In this study, pilot scale tunnel dryers have been investigated to demonstrate the effect of integrating fins. Comparing the results of this work and related studies on large scale tunnel dryers indicates that fin modification can be utilized in large scale dryers to improve the thermal performance. Moreover, in a study done by Panli et al. [63] a large-scale roof drying similar to tunnel dryer has been used for drying sewage sludge.

6. Conclusion

In the current study, a new tunnel type solar tunnel drying system to be utilized in dehumidification of sewage sludge has been investigated experimentally and numerically. Accordingly, three various tunnel dryers have been developed and numerically analyzed. Then, quonset solar tunnel dryer design has been selected and manufactured regarding to the CFD simulation results. The performance tests were done on June and January to specify the overall performance of tunnel dryers. The main outcomes of the present research could be given as:

- Utilizing fin modification in quonset type dryer has considerable positive effect on the thermal performance of the system.
- Adding fins to the drying system reduced the drying time notably.
- Specific moisture extraction rate (SMER) value was achieved between the range of 0.39-0.89 kg/kWh.
- In summer experiments, average COP values for QSTD/F and QSTD were attained between the ranges of 4.28-4.88 and 3.86-4.25, respectively. In winter tests, these values for QSTD/F and QSTD were achieved between the ranges of 3.45-4.08 and 3.11-3.66, respectively.
- EE of the tunnel dryer was averagely increased as 17.2% by utilizing fin modification.

Consequently, quonset form solar absorber can be successfully utilized in various drying applications. Moreover, in future studies, different fin modifications and thermal energy storage units can be integrated to this successful quonset solar tunnel dryer design to enhance the thermal performance.

References

[1] A.D. Tuncer, A. Sözen, A. Khanlari, A. Amini, C. Şirin, Thermal performance analysis of a quadruple-pass solar air collector assisted pilot-scale greenhouse dryer, Solar Energy 203 (2020) 304-316.

[2] F. Afshari, H. Afshari, F. Afshari, H.G. Zavaragh, The effect of nanofilter and nanoclay on reducing pollutant emmisions from rapeseed biodiesel in a diesel engine, Waste and biomass valorization 9 (2018) 1655-1667.

[3] A. Khanlari, A. Sözen, C. Şirin, A.D. Tuncer, A. Gungor, Performance enhancement of a greenhouse dryer: Analysis of a cost-effective alternative solar air heater, Journal of Cleaner Production 251 (2020) 119672.

[4] A. Khanlari, A. Sözen, F. Afshari, C. Şirin, A.D. Tuncer, A. Gungor, Drying municipal sewage sludge with v-groove triple-pass and quadruple-pass solar air heaters along with testing of a solar absorber drying chamber, Science of The Total Environment 709 (2020) 136198.

[5] A.L. Hernández, J.E. Quiñonez, Experimental validation of an analytical model for performance estimation of natural convection solar air heating collectors, Renewable Energy 117 (2018) 202-216.

[6] S.A. Kalogirou, Solar thermal collectors and applications, Progress in energy and combustion science 30 (2004) 231-295.

[7] C. Vassiliades, A. Michael, A. Savvides, S. Kalogirou, Improvement of passive behaviour of existing buildings through the integration of active solar energy systems, Energy 163 (2018) 1178-1192.

[8] M. Esen, H. Esen, Experimental investigation of a two-phase closed thermosyphon solar water heater, Solar Energy 79 (2005) 459-468.

[9] A. Sözen, T. Menlik, S. Ünvar, Determination of efficiency of flat-plate solar collectors using neural network approach, Expert Systems with Applications 35 (2008) 1533-1539.

[10] B. Ameri, S. Hanini, M. Boumahdi, Influence of drying methods on the thermodynamic parameters, effective moisture diffusion and drying rate of wastewater sewage sludge, Renewable Energy 147 (2020) 1107-1119.

[11] İ. Ceylan, A.E. Gürel, Solar-assisted fluidized bed dryer integrated with a heat pump for mint leaves, Applied Thermal Engineering 106 (2016) 899-905.

[12] A. Singh, J. Sarkar, R.R. Sahoo, Experimental performance analysis of novel indirect-expansion solar-infrared assisted heat pump dryer for agricultural products, Solar Energy 206 (2020) 907-917.
[13] E. Veeramanipriya, A.R. Umayal Sundari, Performance evaluation of hybrid photovoltaic thermal (PVT) solar dryer for drying of cassava, Solar Energy 215 (2021) 240-251.
[14] P. Wang, D. Mohammed, P. Zhou, Z. Lou, P. Qian, Q. Zhou, Roof solar drying processes for sewage sludge within sandwich-like chamber bed, Renewable Energy 136 (2019) 1071-1081.
[15] S. Di Fraia, R.D. Figaj, N. Massarotti, L. Vanoli, An integrated system for sewage sludge drying through solar energy and a combined heat and power unit fuelled by biogas, Energy Conversion and Management 171 (2018) 587-603.
[16] A.D. Tuncer, A. Sözen, F. Afshari, A. Khanlari, C. Şirin, A. Gungor, Testing of a novel convex-type solar absorber drying chamber in dehumidification process of municipal sewage sludge, Journal of Cleaner Production 272 (2020) 122862.
[17] P. Krawczyk, 2016. Numerical modeling of simultaneous heat and moisture transfer during sewage sludge drying in solar dryer, Procedia Engineering, 157 (2016) 230-237.
[18] E. Kocbek, H.A. Garcia, C.M. Hooijmans, I. Mijatović, B. Lah, D. Brdjanovic, Microwave treatment of municipal sewage sludge: Evaluation of the drying performance and energy demand of a pilot-scale microwave drying system, Science of the Total Environment 742 (2020) 140541.
[19] E.A. Mewa, M.W. Okoth, C.N. Kunyanga, M.N. Rugiri, Experimental evaluation of beef drying kinetics in a solar tunnel dryer, Renewable energy 139 (2019) 235-241.
[20] A.K., Karthikeyan, S. Murugavelh, Thin layer drying kinetics and exergy analysis of turmeric (Curcuma longa) in a mixed mode forced convection solar tunnel dryer, Renewable Energy 128 (2018) 305-312.
[21] B. Ameri, S. Hanini, A. Benhamou, D. Chibane, Comparative approach to the performance of direct and indirect solar drying of sludge from sewage plants, experimental and theoretical evaluation, Solar Energy 159 (2018) 722-732.

[22] N. Srisittipokakun, K. Kirdsiri, J. Kaewkhao, Solar drying of Andrographis paniculata using a parabolicshaped solar tunnel dryer, Procedia Engineering 32 (2012) 839-846.

[23] M.A. Eltawil, M.M. Azam, A.O. Alghannam, Energy analysis of hybrid solar tunnel dryer with PV system and solar collector for drying mint (MenthaViridis), Journal of Cleaner Production 181 (2018) 352-364.

[24] M.A. Eltawil, M.M. Azam, A.O. Alghannam, Solar PV powered mixed-mode tunnel dryer for drying potato chips, Renewable Energy 116 (2018) 594-605.

[25] M.M. Morad, M.A. El-Shazly, K.I. Wasfy, H.A. El-Maghawry, Thermal analysis and performance evaluation of a solar tunnel greenhouse dryer for drying peppermint plants, Renewable energy 101 (2017) 992-1004.

[26] D.K. Rabha, P. Muthukumar, C. Somayaji, Experimental investigation of thin layer drying kinetics of ghost chilli pepper (Capsicum Chinense Jacq.) dried in a forced convection solar tunnel dryer, Renewable energy 105 (2017) 583-589.

[27] M.S.W. Potgieter, C.R. Bester, M. Bhamjee, Experimental and CFD investigation of a hybrid solar air heater, Solar Energy 195 (2020) 413-428.

[28] N. Kottayat, S. Kumar, A.K. Yadav, S. Anish, Enhanced thermo-hydraulic performance in a V-ribbed triangular duct solar air heater: CFD and exergy analysis, Energy (2020) 117448.

[29] A.K. Raj, M. Srinivas, S. Jayaraj, CFD modeling of macro-encapsulated latent heat storage system used for solar heating applications, International Journal of Thermal Sciences, 139 (2019) 88-104.

[30] K. Nidhul, A.K. Yadav, S. Anish, Arunachala, U.C., Efficient design of an artificially roughened solar air heater with semi-cylindrical side walls: CFD and exergy analysis, Solar Energy 207 (2020) 289-304.

[31] Ansys, ANSYS Fluent Theory Guide, ANSYS Inc, Canonsburg, 2017.

[32] M. Vivekanandan, K. Periasamy, C. Dinesh Babu, G. Selvakumar, R. Arivazhagan, Experimental and CFD investigation of six shapes of solar greenhouse dryer in no load conditions to identify the ideal shape of dryer, Materials Today: Proceedings. doi:10.1016/j.matpr.2020.07.062

[33] J.S. Perret, A.M. Al-Ismaili, S.S. Sablani, Development of a Humidification–Dehumidification System in a Quonset Greenhouse for Sustainable Crop Production in Arid Regions, Biosystems Engineering 91 (2005) 349-359.

[34] D. Jagadeesh, M. Vivekanandan, A. Natarajan, S. Chandrasekar, Experimental conditions to identify the ideal shape of dryer investigation of six shapes of solar greenhouse dryer in no load, Materials Today: Proceedings. https://doi.org/10.1016/j.matpr.2020.05.386.
[35] A.M. Khallaf, M.A. Tawfik, A.A. El-Sebaii, A.A. Sagade, Mathematical modeling and experimental validation of the thermal performance of a novel design solar cooker, Solar Energy 217 (2020) 40-50.
[36] H.Ö. Güler, A. Sözen, A.D. Tuncer, F. Afshari, A. Khanlari, C. Şirin, A. Gungor, Experimental and CFD survey of indirect solar dryer modified with low-cost iron mesh, Solar Energy 197 (2020) 371-384.
[37] T. Seerangurayara, A.M. Al-Ismaili, L.H.J. Jeewantha, A. Al-Nabhani, Experimental investigation of shrinkage and microstructural properties of date fruits at three solar drying methods, Solar Energy 180 (2019) 445-455.
[38] F.J.A. Duffie, W.A. Beckman, Solar Engineering of Thermal Processes, second ed., John Wiley and Sons, New York: USA (1991).
[39] M.G.A. Vieira, L. Estrella, S.C.S. Rocha, Energy efficiency and drying kinetics of recycled paper pulp, Dry. Technol. 25 (2007) 1639-1648.
[40] A.D. Tuncer, A. Khanlari, A. Sözen, E.Y. Gürbüz, C. Şirin, A. Gungor, Energy-exergy and enviro-economic survey of solar air heaters with various air channel modifications, Renewable Energy 160 (2020) 67-85.
[41] Ü. Ağbulut, M. Karagöz, S. Sarıdemir, A. Öztürk, Impact of various metal-oxide based nanoparticles and biodiesel blends on the combustion, performance, emission, vibration and noise characteristics of a CI engine, Fuel 270 (2020) 117521.
[42] A. Sözen, C. Şirin, A. Khanlari, A.D. Tuncer, E.Y. Gürbüz, Thermal performance enhancement of tube-type alternative indirect solar dryer with iron mesh modification, Solar Energy 207 (2020) 1269-1281.
[43] F. Afshari, A. Sözen, A. Khanlari, A.D. Tuncer, C. Şirin, Effect of turbulator modifications on the thermal performance of cost-effective alternative solar air heater, Renewable Energy 158 (2020) 297-310.
[44] F. Nasri, Solar thermal drying performance analysis of banana and peach in the region of Gafsa (Tunisia), Case Studies in Thermal Engineering 22 (2020) 100771.

[45] J.P. Ekka, K. Bala, P. Muthukumar, D.K. Kanaujiya, Performance Analysis of a Forced Convection Mixed Mode Horizontal Solar Cabinet Dryer for Drying of Black Ginger (Kaempferia Parviflora) using Two Successive Air Mass Flow Rates, Renewable Energy 152 (2020) 55-66.
[46] F. Ullah, M. Kang, Impact of air flow rate on drying of apples and performance assessment of parabolic trough solar collector, Applied Thermal Engineering 127 (2017) 275-280.
[47] M.U.H. Suzihaque, R. Driscoll, Effects of Solar Radiation, Buoyancy of Air Flow and Optimization Study of Coffee Drying in a Heat Recovery Dryer, Procedia Engineering 148 (2016) 812-822.
[48] M. Yahya, A. Fudholi, K. Sopian, Design and performance of solar-assisted fluidized bed drying of paddy, Res J Appl Sci Eng Technol 12 (2016) 420-426.
[49] M. Yahya, Design and performance evaluation of a solar assisted heat pump dryer integrated with biomass furnace for red chilli, Int J Photoenergy (2016) 1-14.
[50] M. Dorouzi, H. Mortezapour, H.R. Akhavan, A.G. Moghaddam, Tomato slices drying in a liquid desiccant-assisted solar dryer coupled with a photovoltaic-thermal regeneration system, Solar Energy 162 (2018) 364-371.
[51] A. Fudholi, K. Sopian, M.Y. Othman, M.H. Ruslan, Energy and exergy analyses of solar drying system for red seaweed, Energy Build 68 (2014) 121-129.
[52] A. Fudholi, K. Sopian, M.H. Yazdi, M.H. Ruslan, M. Gabbasa, H.A. Kazem, Performance analysis of solar drying system for red chili, Sol Energy 99 (2014) 47-54.
[53] A. Khanlari, A.D. Tuncer, A. Sözen, C. Şirin, A. Gungor, Energetic, environmental and economic analysis of drying municipal sewage sludge with a modified sustainable solar drying system, Solar Energy 208 (2020) 787-799.
[54] V. Shanmugam, E. Natarajan, Experimental investigation of forced convection and desiccant integrated solar dryer, Renew Energy 31 (2006) 1239-1251.
[55] M. Mohanraj, P. Chandrasekar, Comparison of drying characteristics and quality of copra obtained in a forced convection solar drier and sun drying, J Sci Ind Res 67 (2008) 381-385.
[56] M. Mohanraj, P. Chandrasekar, Performance of a forced convection solar drier integrated with gravel as heat storage material for chili drying, J Eng Sci Technol 4 (2009) 305-314.

[57] A. Fudholi, M.Y. Othman, M.H. Ruslan, K. Sopian, Drying of Malaysian Capsicum annuum L. (red chili) dried by open and solar drying, Int J Photoenergy (2013) 1-9.

[58] A. Fudholi, K. Sopian, M.A. Alghoul, M.H. Ruslan, M.Y. Othman, Performances and improvement potential of solar drying system for palm oil fronds, Renewable Energy 78 (2015) 561-565.

[59] M. Balbine, E. Marcel, K. Alexis, Z. Belkacem, Experimental evaluation of the thermal performance of dryer airflow configuration, Int. J. Energy Eng. 5 (2015) 80-86.

[60] N.S. Rathore, N.L. Panwar, Design and development of energy efficient solar tunnel dryer for industrial drying, Clean Technologies and Environmental Policy 13 (2011), 125-132.

[61] E.A. Mewa, M.W. Okoth, C.N. Kunyanga, M.N. Rugiri, Experimental evaluation of beef drying kinetics in a solar tunnel dryer, Renewable Energy 139 (2019) 235-241.

[62] M.S. Seveda, Performance studies of solar tunnel dryer for drying aonla (embilica officinalis) pulp, Applied Solar Energy, 48(2), (2012) 104-111.

[63] W. Panli, M. Danish, Z. Pin, L. Ziyang, Q. Pansheng, Z. Quanfa, Roof solar drying processes for sewage sludge within sandwich-like chamber bed, Renewable Energy 136 (2018) 1071-1081.